Parametric study of the progressive collapse of 2D framed structures

Enrico Masoero[1], Falk K. Wittel[2], Bernardino M. Chiaia[1], Hans J. Herrmann[2]
[1]*Department of Structural Engineering, Politecnico di Torino, Italy*
E-mail: enrico.masoero@polito.it, bernardino.chiaia@polito.it

[2]*Department of Building Materials, Swiss Federal Institute of Technology ETH Zurich, Switzerland*
E-mail: fwittel@ethz.ch, hans@ifb.baug.ethz.ch

Keywords: Structural mechanics, 2D framed structures, progressive collapse, robustness, discrete elements method.

SUMMARY. In this paper we study the response of 2D framed structures made of reinforced concrete to the sudden removal of columns. For comparative reasons, the 2D frames are considered as part of 3D structures with same overall structural mass and external load potential. In particular, we study two sets of 2D frames, with different height-bay ratio λ of the structural cells. Each set counts 3 frames with different hierarchical level n, defining structures that range from hierarchical to homogeneous. Hierarchical structures have massive primary structure consisting of few large elements while homogeneous structures are made of many thin structural elements. Employing an algorithm based on Discrete Elements, we simulate progressive collapse until the final stage, considering collisions between the structural elements and with the ground. We point out the mechanisms that trigger progressive collapse when the columns are strong and when they are weak. We quantify the robustness in terms of Reserve Strength Ratio RSR and show the influence of λ and n on the RSR, that depends on the activated collapse mechanism and on the extent of the initial damage.

1 INTRODUCTION

Local accidental damage to structures can lead to catastrophic scenarios if progressive collapse is triggered [1]. The ability of a system to prevent damage spreading is called *robustness* and is a necessary requirement for large buildings. Presently, many measures to avoid progressive collapse are known and under discussion. These measures generally involve either the concept of redundancy or that of compartmentalization. Providing redundancy means activating a large number of structural elements in the stress redistribution process triggered by local damage. In this sense, structures made of many tough elements, with tough connections and reinforced by ties are preferred. On the other hand, compartmentalizing a structure means subdividing it into statically independent portions so that, if some are damaged and collapse, the neighbouring portions will not be torn down along with the collapsed ones. Comparmentalization can be achieved by strategically arranging brittle structural elements and connections. These measures require local interventions and neglect the role of the overall structural geometry towards the response to local damage. Nevertheless, choosing optimal geometries is advantageous since it permits to maximize structural robustness at the design stage prior to improving it with specific local interventions. Some studies in the topic of structural optimization towards damage can be found in the field of Fracture Mechanics, where e.g. [2] showed that cellular structures are more tolerant to local flaws if their cells are triangular or hexagonal rather than rectangular.

In this work we focus on the effect of structural geometry on robustness, and precisely we answer to two questions. The first one is whether a *homogeneous* structure, made of many thin beams and

columns, is more robust than a *hierarchical* one, with strong massive primary structure supporting a weak secondary structure considered as external load. The second question is whether the height-bay aspect ratio of the rectangular structural cells of regular framed structures influences the robustness. In order to answer to these questions, we perform simulations on 2D framed structures made of reinforced concrete and damaged by the removal of structural elements contained inside a damage area, according to the Alternate Load Path Method Approach (ALPM) [3]. In Section 2 we describe the frames and define the initial damage area. The numerical algorithm based on Discrete Elements (DE) that we employed for the simulations is described in Section 3. We finally show and discuss the results of the simulations in Section 4.

2 DESCRIPTION OF THE STRUCTURES

We construct two sets of regular 2D frames made of reinforced concrete (RC). The mechanical parameters of concrete and steel are shown in Table 1. The frames have same total height $H_{tot} =$ 33m (see Figure 1) and different height-bay aspect ratio $\lambda = H/L$ of the structural cells. Namely, $\lambda = 0.75$ for the first set and $\lambda = 1.33$ for the second one. Each set consists of three frames with identical total width L_{tot} and different *hierarchical level* n. n^2 is actually the number of structural cells in a frame and we call a structure *hierarchical* when n is small and *homogeneous* when n is large. The frames with $n = 2$ and $n = 5$ represent a reorganization of those with $n = 11$ aimed at creating a more massive primary structure supporting a thin secondary structure (see Figure 1). We neglect stiffness and strength of the secondary structure that we consider just as an additional external load. Following this principle, we now explain how we obtain the geometry and the loads of the frames with $n = 2$ and $n = 5$ starting from the frames with $n = 11$.

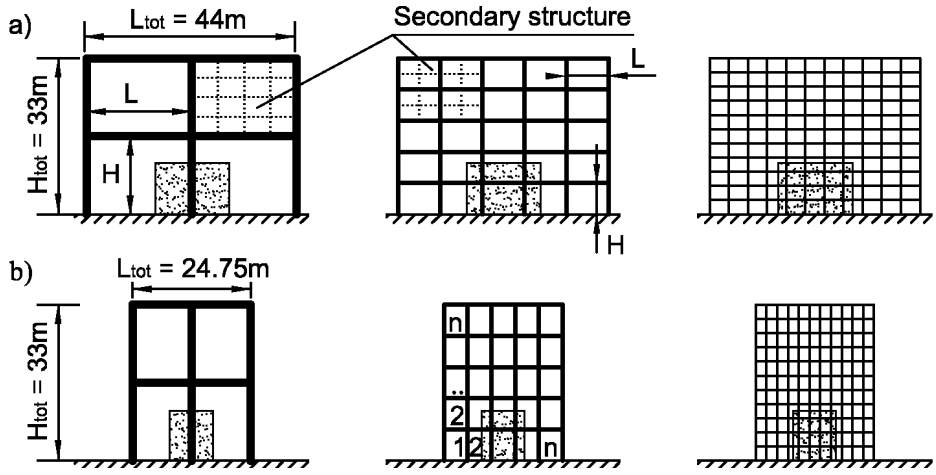

Figure 1: Studied 2D frames with a) $\lambda = 0.75$ and b) $\lambda = 1.33$. The dotted region is the damage area. The cohesion of the elements inside this area is suddenly removed to represent the initial accidental damage.

For what concerns the geometry, each floor and column of the $n = 5$ frames corresponds to two

floors and columns of the $n = 11$ frames, except for the first floor slab of the $n = 11$ frame. This first floor slab is simply deleted since it corresponds to a part of secondary structure in the $n = 5$ frame that is directly carried by the ground (see Figure 1). The same procedure permits to obtain the geometry of the frames with $n = 2$ starting from those with $n = 5$.

Parameter	*Symbol*	*Units*	*Value*
RC, specific weight	γ_{RC}	kg/m^3	2500
RC, Young modulus	E_c	N/m^2	$30{\cdot}10^9$
RC, compressive yield stress (Section 4.1)	f_c	N/m^2	$35{\cdot}10^6$
RC, compressive yield stress (Section 4.2)	f_c	N/m^2	$0.35{\cdot}10^6$
RC, ultimate shortening	$\epsilon_{u,c}$	$-$	0.0035
Steel, Young's modulus	E_s	N/m^2	$200{\cdot}10^9$
Steel, yield stress	f_y	N/m^2	$440{\cdot}10^6$
Steel, ultimate strain	$\epsilon_{u,s}$	$-$	0.05

Table 1: Mechanical properties of reinforced concrete and steel.

The damage areas (dotted in Figure 1) contain the structural elements that are initially removed to represent an accidental damage event. The damage area is the same for frames with same λ, so that the columns and beams removed from frames with $n = 11$ correspond to the structural elements removed from frames with $n = 5$ and $n = 2$. In this way we represent accidental damage events with a given amount of destructive energy or spatial extent, like explosions or impacts. Very local damage events like gross errors would be better represented by the removal of single elements. Here we don't perform simulations with very local damage events, but we discuss their effect in Sections 4.1 and 4.2 referring to the results shown in this paper and to those obtained in [4].

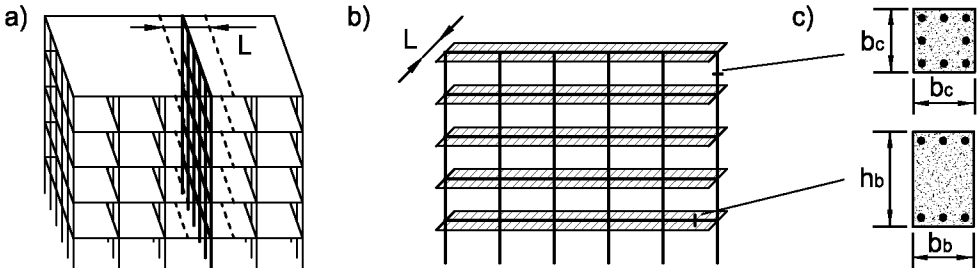

Figure 2: a) Typical 3D structure and selected 2D frame; b) typical 2D frame with corresponding loaded portion of floor slabs (dashed region); c) cross sections of columns and beams.

In order to define the cross sectional features of the structural elements and the load, we consider the 2D frame as part of a 3D regular framed structure with $n \times n \times n$ cells (see Figures 2.a and 2.b). The cross section of the columns is square, with edge b_c proportional to H with factor λ_c.

The beams have rectangular cross section whose height h_b is proportional to L with factor λ_b and whose base b_b is proportional to h_b with aspect ratio coefficient δ_b (see Figure 2.c and Table 2). The area of reinforcement A_s is proportional to the area of the cross section with factor ρ_s (see Table 2) and is arranged as shown in Figure 2.c. The thickness h_s of the floor slabs of the 3D structure is proportional to L with factor λ_s. Differently from λ_c and λ_b, λ_s is not constant but decreases with L. This assumption is justified by the fact that large floors generally do not consist of a homogeneous slab in RC but are lighter composite structures. Thus the thickness of an equivalent slab grows less than proportionally to the bay. We adopt the expressions for λ_s shown in Table 2 to guarantee that the total mass of the structural elements of a 3D framed structure with given overall size H_{tot} and L_{tot} and slenderness of the cell λ does not depend on n. In this way, we can compare the performances of frames whose primary structures have the same mass.

$Parameter$	$Symbol$	$Units$	$Value, \lambda = 0.75$	$Value, \lambda = 1.33$
Slenderness of the columns	λ_c	$-$	$1/10$	
Slenderness of the beams	λ_b	$-$	$1/10$	
Slenderness of the slabs	λ_s	$-$	$1/20 - \chi(L - L_{n=11})$	
Aspect ratio of the beams	δ_b	$-$	$2/3$	
Fraction of reinforcement (columns)	$\rho_{s,c}$	$-$	0.0226 ($8\phi18$ for n=11)	
Fraction of reinforcement (beams)	$\rho_{s,b}$	$-$	0.0029 ($4\phi14$ for n=11)	
Bay of the structural cell when n=11	$L_{n=11}$	m	4	2.25
χ factor for slabs slenderness	χ	$-$	0.00055	0.003

Table 2: Geometric parameters of the cross sections.

We consider a uniformly distributed external load at each floor of the 3D secondary structure. The external load on frames with $n = 11$ consists of a dead load $G = 2850\text{N/m}^2$ due to internal walls, pavements, plaster, etc., plus a live load $Q = 2000\text{N/m}^2$. Differently, the primary structures represented by frames with $n = 5$ and $n = 2$ support 3 and 1 floors of secondary structure respectively. Therefore the external load carried by the primary structures is $4 \cdot (G + Q)$ when $n = 2$ and $2 \cdot (G + Q)$ when $n = 5$. This load scaling provides a constant total potential energy of the external load on undeformed structures with different n and same λ.

Considering now the 2D frame in Figure 2.b, the external load per unit length on the beams is obtained multiplying the load per unit area with L. We convert the load into an extra mass per unit length by dividing it by the gravity acceleration. Furthermore, an additional extra mass per unit length on the 2D frames comes from the floor slabs of the 3D frames. For frames with $n = 11$, this additional extra mass is $\gamma_{RC} h_s L$, where γ_{RC} is the specific weight of RC (see Table 1). According to the principle that we followed for the external load, we set the extra mass given by the floor slabs on the primary structures to $4 \cdot (\gamma_{RC} h_s L)$ for frames with $n = 2$ and to $2 \cdot (\gamma_{RC} h_s L)$ for frames with $n = 5$. In this way we overestimate the weight of the secondary structure's floor slabs, since their bay is smaller than that of the floor slabs of the primary structure. We also neglect the beneficial load carrying contribution of the primary floor slabs since we consider them just as an external load on the 2D frames. Overestimating the weight of the secondary floor slabs and neglecting the load carrying contribution of the primary floor slabs leads to underestimate of the strength of the 2D frame as part of a 3D system. Nevertheless, in Section 4.1 we explain why we don't expect these assumptions to

significantly affect the robustness indicator we refer to.

3 MODEL DESCRIPTION

The Discrete Elements model that we use in this work is based on [5]. We subdivide the columns and the beams of the 2D frames in 10 linear elastic - perfectly plastic Euler-Bernoulli (EB) beam elements, with ultimate elongation and rotation threshold. The linear elastic regime of the EB elements is described in [6]. Damping is applied to the elastic part of the elongation and the bending strain by means of the damping coefficients γ_L and γ_B (see Table 3).

$Parameter$	$Symbol$	$Units$	$Value, \lambda = 0.75$			$Value, \lambda = 1.33$		
			n=2	n=5	n=11	n=2	n=5	n=11
EB element elongation damping	γ_L	Ns/m	100	100	100	100	100	100
EB element bending damping	γ_B	Nms	100	10	10	100	10	10
EB. el. elongation threshold	ε^{th}	$-$	$= \varepsilon_{u,s}$					
EB. el. shortening threshold	ε_c^{th}	$-$	$= \varepsilon_{u,c}$					
EB. el. plastic rotation threshold	φ^{th}	rad	0.1					
$Sphere - sphere\ Hertz\ coefficients$								
Stiffness	Y	$10^7 N/m^3$	10	2	0.5	10	2	0.5
Normal damping coefficient	γ_n	$10^6 Ns/m$	10	2	0.2	10	2	0.2
Tangent damp. coef. (Coulomb)	μ	$10^4 Ns/m$	1	1	1	1	1	1
Tangent damp. coef. (dynamic)	γ_t	$10^4 Ns/m$	1	1	1	1	1	1
Rolling damping coef.	γ_w	Nms	50	50	50	50	50	50
$Sphere - ground\ Hertz\ coefficients$								
Stiffness	Y^g	$10^7 N/m^3$	5	5	5	5	5	5
Normal damping coefficient	γ_n^g	$10^6 Ns/m$	5	1	1	5	1	1
Tangent damp. coef. (Coulomb)	μ^g	$10^4 Ns/m$	5	5	5	5	5	5
Tangent damp. coef. (dynamic)	γ_t^g	$10^4 Ns/m$	5	5	5	5	5	5

Table 3: Damping coefficients and ultimate thresholds of the EB elements. Hertzian contact parameters.

The plastic regime can be entered because of axial force N or bending moment B. For the sake of simplicity, we consider uncoupled plasticity in bending and in axial direction. Therefore, axial plasticity occurs when the axial force inside the EB element overcomes the compression or the tension yield threshold N_c^y and N^y (see Table 3). If this happens, an additional compressive or tensile strain ε^{pl} is added to restore $N = N_c^y$ or $N = N^y$. We set $N^y = A_s f_y$ referring to the yield strain of steel f_y and neglecting the contribution of concrete in tension. $N_c^y = A^e f_c$ refers to the compressive strength of concrete f_c and neglects the contribution of steel under compression. The bending moment B_i at the i^{th} edge node of an EB element ($i = 0, 1$) overcomes the yield threshold B^y, an additional plastic rotation φ_i^{pl} is added at node i to restore $|B_i| = B^y$. It is worth noting that adding a plastic rotation e.g. at node 0 modifies either B_0 and B_1. If B^y is overcome at both the edge nodes 0 and 1, additional plastic rotations are added at both nodes, still in order to obtain

$|B_0| = B^y$ and $|B_1| = B^y$. Neglecting the contribution of concrete, we set B^y to:

$$B^y = t_s^e \rho_s^e A^e f_y h^e + \Delta B^y, \tag{1}$$

where the superscript e means that we refer to the generic EB element, that can be a segment of either a column or a beam. In (1), t_s is the fraction of reinforcement in tension, i.e. $\frac{3}{8}$ for the columns and $\frac{1}{2}$ for the beams (see Fig. 2.c), A and h are the area and the height of the cross section, and ΔB^y takes into account the beneficial effect on B^y brought by compression inside the EB element. We set ΔB^y imposing:

$$-\frac{N}{A^e E_c} = \frac{\Delta B^y}{t_s^e \rho_s^e A^e h^e E_s}, \tag{2}$$

where E_c and E_s are the Young's moduli of concrete and steel. If the plastic elongation and rotations satisfy the breaking rules:

$$\frac{\varepsilon^{pl}}{(\varepsilon^{th} - \varepsilon^y)} + max\frac{|\varphi_i^{pl}|}{\varphi^{th}} \geq 1 \qquad for \;\; \varepsilon^{pl} > 0, \tag{3}$$

$$-\frac{\varepsilon^{pl}}{|\varepsilon_c^{th} - \varepsilon_c^y|} + max\frac{|\varphi_i^{pl}|}{\varphi^{th}} \geq 1 \qquad for \;\; \varepsilon^{pl} < 0, \tag{4}$$

the element is considered to fail and is thus immediately removed from the system. In (3) and (4), ε^{th} and ε_c^{th} are the elongation breaking threshold of an EB element in tension and compression. φ^{th} is the ultimate plastic rotation. $\varepsilon^y = N^y/(E_c A^e)$ and $\varepsilon_c^y = N_c^y/(E_c A^e)$ are the axial strain corresponding to tensile and compressive yielding.

We represent the volume of the structural elements by disks surrounding each node. The diameter of the k^{th} disk is equal to 80% of the length of the shortest EB element connected to node k. The mass M_k is obtained summing the contributions from the mass of the EB elements connected to node k and from an extra mass given by the external load and the floor slab (see Section 2). The rotational inertia of a disk is computed considering M_k being uniformly distributed.

Therefore, the generic k^{th} node is subjected to the effect of the gravity acceleration on M_k and to forces transmitted by the EB elements connected to it. The dynamics of the system is described by means of a direct time integration 5^{th} order Gear Predictor-Corrector algorithm, with time step $1 \cdot 10^{-6}$s. The failure of a sufficiently large number of EB element can disconnect portions of the structure that fall and can collide with other structural elements or with the ground. Collisions are considered by means of Hertzian overlapping, i.e. repulsive and tangential forces are added to nodes whose surrounding disks partially overlap [6]. The contact forces are proportional to the overlapping area and to the relative velocities of the colliding disks with stiffness modulus Y and damping coefficients (see Table 3).

4 SIMULATIONS AND RESULTS:

We run the simulations scaling the external load and the self weight of the frames by a load multiplier μ, which is the control parameter of our system. Given μ, we initially set the frames to static equilibrium. Then we apply the initial damage removing the EB elements inside the damage area (see Figure 1) and we simulate the subsequent dynamic response. We vary μ between a minimum value μ_c and a maximum value μ_u. μ_c is the largest load multiplier for which the damaged structure does not suffer any further failure after the initial damage. When $\mu < \mu_c$ the frame is perfectly robust towards the initial damage. μ_u is the smaller load multiplier for which the structure collapses

before the initial damage. When $\mu > \mu_u$ the intact structure collapses before attaining static equilibrium and thus is unable to carry the scaled service load. When $\mu_c < \mu < \mu_u$ the structure undergoes progressive collapse after the initial damage. Depending on the activated collapse mechanism, on the collapse evolution and on n, the final outcome can be partial or total collapse. We quantify the structural robustness of the frames evaluating the Reserve Strength Ratio RSR:

$$RSR = \frac{\mu_c}{\mu_u}. \tag{5}$$

In the following we discuss the influence of λ and n on μ_c, μ_u and on the RSR. In particular, in Section 4.1 we study frames with columns that are stronger than the beams. In this case after the initial damage the beams above the damage area fail in bending and trigger progressive collapse. In Section 4.2, we consider frames with weak columns that, after the initial damage, progressively fail under compression triggering pancake collapse.

4.1 *Bending collapse mechanism*

The results shown in this Section refer to the frames described in Section 2 and for which we set the compressive strength of the RC to $f_c = 35$N/mm^2. This value of f_c leads to frames with strong columns.

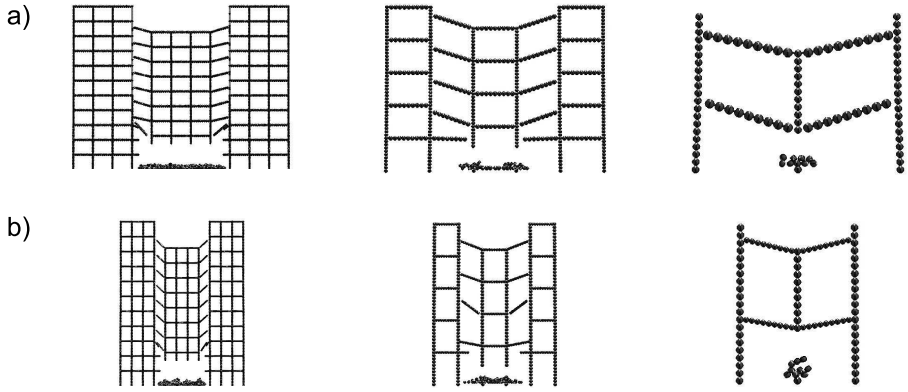

Figure 3: Bending collapse of the studied 2D frames with a) $\lambda = 0.75$ and b) $\lambda = 1.33$ for n=2,5,11.

These frames collapse after the initial damage if bending failure of the beams above the damage area is triggered (see Figure 3).The bending collapse mechanism is local since it only involves the portion of structure directly above the damage area. Nevertheless, if μ is sufficiently large and still smaller than μ_u, the horizontal forces exerted by the falling central portion of the structure on the lateral portions can tear these latter down (see Figure 4) until total collapse. We call μ_{pt} the smallest μ for which this secondary mechanism is activated. This mechanism relies on the plastic properties of the structural elements and thus can be avoided by opportunely compartmentalizing the structure. Of course, frames with $n = 2$ can only experience total collapse after the bending mechanism is

triggered and thus for them $\mu_{pt} = \mu_c$.

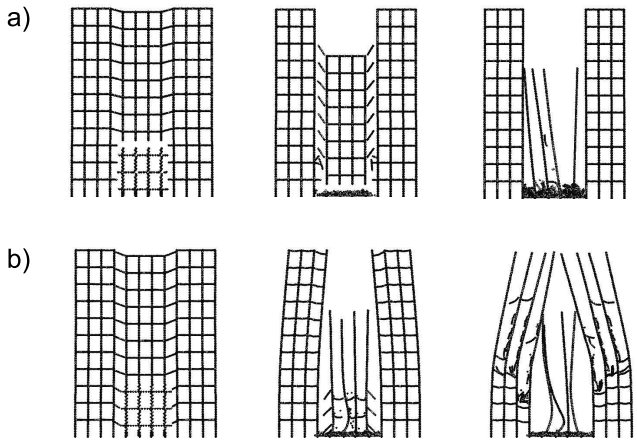

Figure 4: Snapshots of the a) partial and b) total collapse of frames with $\lambda = 1.33$, after the triggering of a bending mechanism.

Figure 5 shows that λ has beneficial effects on the strength of the structure, i.e on the μ values. This result agrees with the results in [4], obtained by means of linear elastic static analyses. Differently, hierarchical structures (small n) are less strong than homogeneous ones (large n), but according to the assumptions that we discussed at the end of Section 2 we expect that hierarchical structures can actually be stronger than what this result indicates. Of course, what is interesting in Figure 5 are the trends of μ_c, μ_{pt} and μ_u, since their absolute value can be increased employing stronger structural elements.

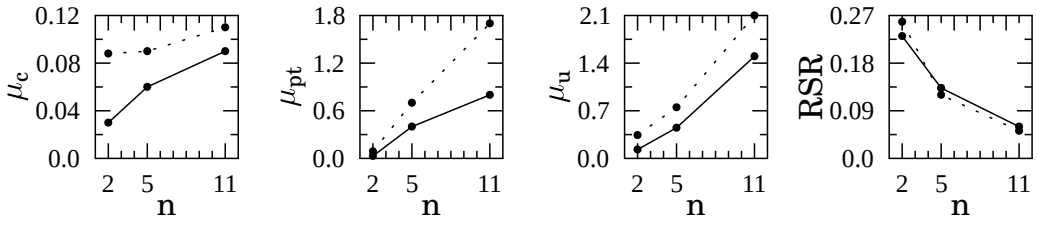

Figure 5: Relevant load multipliers μ and RSR for frames that undergo progressive collapse after bending failure of the beams. The continuous lines refer to $\lambda = 0.75$, the dashed lines to $\lambda = 1.33$.

Figure 5 also shows that the RSR is not influenced by λ and grows as n decreases. Therefore, hierarchical structures are more robust than homogeneous ones towards accidental damage events

with given destructive energy or spatial extent. In this case, we don't expect that the assumptions discussed at the end of Section 2 as well as the eventual employment of stronger structural elements can significantly change the values of the RSR that we obtained. The reason is that if the structural elements are stronger, either μ_c and μ_u grows and thus, according to (5), we expect a compensative effect on the final value of the RSR. The RSR is larger in hierarchical structures because when a bending collapse mechanism occurs, the entity of the stress redistribution inside the beams above the damage area depends on the *number* of columns that are lost at a storey n_{lc}. This is due to the fact that the inter-columns bay in the intact structure is L while in the damaged structure it is $L \cdot (n_{lc}+1)$. Therefore, in agreement with [7], we expect that the hierarchical level n does not influence the RSR when a bending collapse mechanism is triggered by a single column removal.

4.2 *Pancake collapse*

Now we consider the same frames analysed in Section 4.1 but we set the compressive strength of the RC to a very small value, i.e. $f_c = 0.35\text{N/mm}^2$. In this way, the columns get much weaker than the beams. The frames undergo total pancake collapse triggered by progressive failure of the columns under compression (see Figure 6). We adopt such an extremely small value of f_c because this is the simplest way to implement systems where the columns are much weaker than the beams. We could have obtained the same result by reducing the cross section of the columns or increasing the reinforcement or the cross sections of the beams.

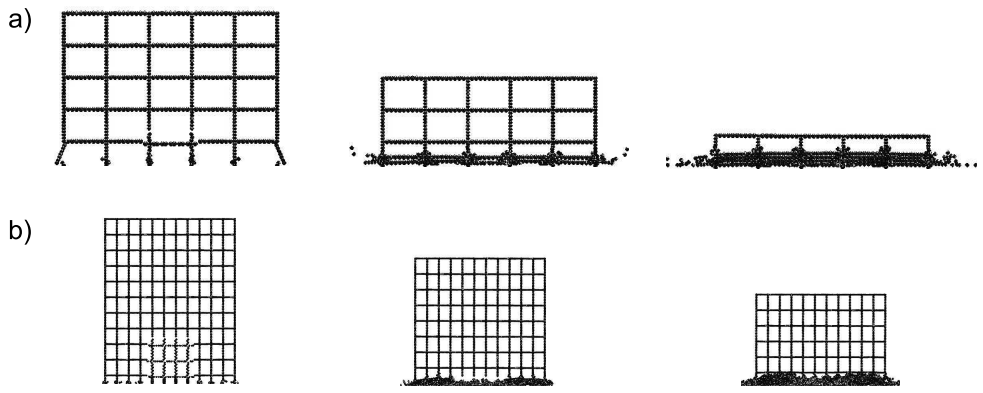

Figure 6: Snapshots of the pancake collapse of frames with a) $\lambda = 0.75$ and b) $\lambda = 1.33$.

The results show that neither the hierarchical level n nor λ influence the RSR in this case. When pancake collapse is triggered, the RSR only depends on the *fraction* of columns that are lost at one storey f_{lc}. In our simulations we always remove $1/3$ of the columns at the first three storeys (see Figure 1) and thus we always obtain $RSR = 0.55 - 0.65$. Therefore, hierarchical and homogeneous structures are equally robust towards pancake collapse triggered by a damage event with given destructive power or spatial extent. Differently, if a single column is lost after a very local damage event, we expect homogeneous structures to be more robust since f_{lc} would be smaller for them. Finally, it is worth noting that the RSR towards pancake collapse is remarkably higher than

the RSR towards bending failure (cf. Figure 5). If the beams would be infinitely stiff, we would expect $RSR = 1 - f_{lc}$ that in our case would lead to $RSR = 2/3$. We obtained a slightly smaller RSR because the bending compliance of the beams produce a higher stress concentration inside the columns that are closer to the initial damage area (see [4]).

5 CONCLUSIONS

Regular framed structures with small height-bay aspect ratio λ of the structural cells are less strong than structures with high λ. Nevertheless, λ does not influence the robustness towards the initial removal of structural elements, measured by the Reserve Strength Ratio RSR. The influence of the hierarchical level n on the RSR depends on the collapse mechanism that can be activated. If the structure collapses because of a bending mechanism, the RSR depends on the number of columns that are lost at a storey. Therefore, if the initial damage has a given destructive power or spatial extent like explosions or impacts, hierarchical structures are more robust than homogeneous ones. Differently, if the initial damage brings to the loss of a single column, hierarchical and homogeneous structures are equally robust. If the structure undergoes pancake collapse triggered by progressive failure of the columns under compression, the RSR depends on the fraction of columns that are lost at a storey. In this case, hierarchical and homogeneous structures are equally robust towards initial damage with given spatial extent, while homogeneous structures are more robust towards the loss of a single column. Bending or pancake collapse as well as intermediate mechanism involving both can be activated depending on the relative strength of columns and beams in the structure. Nevertheless, since the RSR towards pancake collapse is remarkably larger than the RSR towards bending collapse mechanisms, hierarchical structures should be preferred in robustness oriented design.

References

[1] Levy, M. and Salvadori, M., *Why Buildings Fall Down?*, W. W. Norton, New York (1992).

[2] Chen, J.Y., Huang, Y. and Ortiz, M., "Fracture analysis of cellular materials: a strain gradient model", *J. Mech. Phys. Solids*, **46**, 789-828 (1998).

[3] Val, D.V. and Val, E.G., "Robustness of framed structures", *Struct. Eng. Int.*, **16**, 108-112 (2006).

[4] Chiaia, B.M. and Masoero, E., "Structural robustness: the role of geometry and complexity and the brittle fracture analogy", in *Proc. Aimeta 2007, 18 Congresso dell'Associazione Italiana di Meccanica Teorica e Applicata*, Brescia, Italy, September 11-14, 2007.

[5] Carmona, H.A., Wittel, F.K., Kun, F. and Herrmann H.J., "Fragmentation processes in impact of spheres", *Phys. Rev. E*, **77**, 243-253 (2008).

[6] Pöschel, T. and Schwager, T., *Computational Granular Dynamics*, Springer-Verlag GmbH, Berlin (2005).

[7] Chiaia, B.M. and Masoero, E., "Analogies between progressive collapse of structures and fracture of materials", *Int. J. Fract.*, **154**, 177-193 (2008).